Int. J. Electrochem. Sci., 17 **(2022)** Article Number: 221277, doi: 10.20964/2022.12.68

International Journal of
ELECTROCHEMICAL
SCIENCE
www.electrochemsci.org

Modelling and Simulation of Microbial Activity in Stratified and Homogeneous Biofilms: Hyperbolic Function Method

J. Saranya[1], *P. Jeyabarathi*[2], *L. Rajendran*[3,*], *M.E.G. Lyons*[4,*]

[1] Department of Mathematics, Mother Terasa Womens University,Kodaikanal, India.
[2] Department of Mathematics, Bharath Institute of Higher Education and Research, Chennai,India
[3] Department of Mathematics, AMET (Deemed to be university), Chennai, India.
[4] School of Chemistry and AMBER National Centre, University of Dublin, Trinity College Dublin, Dublin 2, Ireland
[*]E-mail: raj_sms@rediffmail.com, melyons@tcd.ie

Received: 2 October 2022 / *Accepted:* 20 November 2022 / *Published:* 27 December 2022

The mathematical models of microbial activity in stratified and homogeneous biofilms are discussed. The model is based on a nonlinear equation with a nonlinear term related to the reaction's rate. The time-independent nonlinear equation is solved using the hyperbolic function method. The analytical expression of nutrient concentration and the effectiveness factor in a stratified and homogeneous biofilm are obtained for all values of parameters. The effect of the Thiele modulus, the diffusivity ratio between the surface and the bottom of the biofilm and the effective diffusivity at the bottom of the biofilm on concentration are discussed. Numerical results (Matlab) are used to validate the analytical results, and there is a reasonable level of agreement.

Keywords Mathematical model, Stratified biofilms, Homogeneous biofilm, Hyperbolic function method, Nonlinear equation.

1. INTRODUCTION

Biofilms are complex microbial ecosystems in which multiple physical, chemical, and biological processes simultaneously occur. Depending on the environment, the biofilm may also contain non-cellular elements such as blood components, corrosion particles, clay or silt particles, or mineral crystals. Biofilms commonly have interfaces between solid-liquid, liquid-air, liquid-liquid and solid-liquid media, and they frequently contain one or more microbial species.

Several methods can assess biofilm activity. The method chosen to assess biofilm activity is determined by the nature of the study and usually by analytical convenience. Continuous monitoring of the biofilm formation rate is necessary for many applications. Among the methods used are optical microscopy [1], measuring the amount of light reflected from microbial colonized surfaces [2], gathering and analyzing the images of biofilm depositions [3], surface sensors based on piezoelectric devices [4], and electrochemical sensors in which stainless steel electrodes change their electrochemical behaviour as a result of biofilm deposition [5,6]. Sultana et al. [7] reviewed the electrochemical control of biofilm.

The conceptual model of homogeneous biofilms shown in Figure 1A was used to construct the earliest biofilm models [8, 9]. These models were created to predict the steady-state rates at which biofilms use the nutrients. Numerous scholars modified this model, adding new processes to the fundamental one of steady-state mass transfer. Rittmann and McCarty [10,11] developed their model to include dual nutrition limits and unstable states after introducing bacterial growth and decay factors for a steady-state biofilm. Many biofilm processes have used this paradigm with only minimal alterations

The research community benefited greatly from the homogeneous biofilm model. However, as time progressed, tools for directly quantifying intra-biofilm processes developed, such as confocal microscopy and microelectrodes. It soon became apparent that the biofilm model could not explain some of the experiment results, which assume that microbes are evenly distributed throughout a composite phase of extracellular polymers. New heterogeneous biofilm conceptual models (Fig. 1C) were developed to depict the reality that biofilm microorganisms are densely packed in microcolonies separated by intermediate spaces.

As the heterogeneous biofilm conceptual model became more popular, new mathematical models of microbial activity and accumulation were required. A cellular automata model by Hermanowicz [12] was only meant to represent the most basic case of a single-species biofilm with a single growth-limiting nutrient. Researchers initially created the concept of the localized mass transport coefficient to analyze variations in mass transport rates in heterogeneous biofilms. Later, Beyenal et al. [13] extended this method and evaluated the effective diffusivities in heterogeneous biofilms on a local and surface-averaged level [14,15].

Based on cellular automata, Beyenal et al. [13] established mathematical models of microbial activity in diverse biofilms. The model divides heterogeneous biofilms into layers, with calculations based on each layer's average effective diffusivity and biofilm density. The mean effective diffusivity changes linearly in heterogeneous biofilms and drops off toward the bottom. Since homogeneous biofilms don't exist, their characteristics must be inferred. Homogeneous biofilm activity may be lower, greater, or identical to stratified biofilm activity. Stratified biofilms with high effective diffusivity gradients had lower activities than homogeneous biofilms having average effective diffusivity. According to the model, the growth-limiting nutrient should permeate stratified biofilms more deeply than homogeneous biofilms.

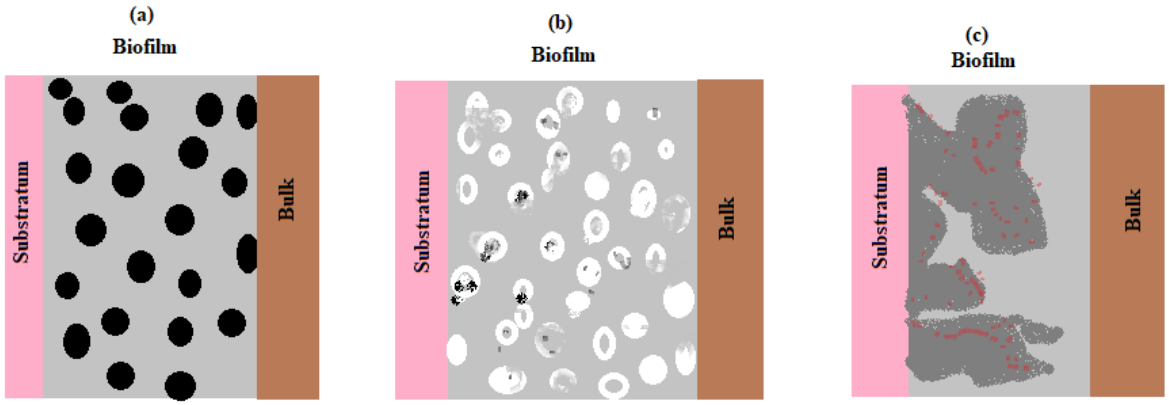

Figure 1. Conceptual models of biofilms. (a) homogenous biofilms, a uniform extracellular polymer matrix, and homogeneously dispersed biomass, (b) multi-species, multi-nutrient biofilm. (c) heterogeneous biofilm formed of microcolonies of concentrated, non-uniformly dispersed biomass that are separated apart voids [13].

This communication discusses the mass transport and microbial activity in a stratified and homogeneous biofilm. The simple analytical expression of concentration profiles and efficiency factors in stratified and homogeneous biofilms is derived by solving nonlinear equations using the hyperbolic function approach, a simple and powerful new algebraic method.

2. MATHEMATICAL FORMULATION OF THE PROBLEM

The nutrient continuity equation in stratified biofilm can be written as follows [13]:

$$D_{fz}\frac{d^2C(z)}{d\,z^2}+\zeta\frac{d\,C(z)}{d\,z}=\frac{\mu_{max}C(z)\,X_{f1}}{Y_{X/S}(K_S+C(z))} \quad (1)$$

where $D_{fz}$is the surface average relative effective diffusivity, D_{fav} is the average effective diffusivity, $C(z)$ is the concentration of growth-limiting nutrient, ζ is the effective diffusivity gradients, $\mu_{max}$is the maximum specific growth rate, X_{f1} is the averaged biofilm density, $Y_{X/S}$ is the yield coefficient, and K_S is the Monod half rate constant. For homogeneous biofilms ($\zeta = 0$), Eq. (1) becomes,

$$D_{fav}\frac{d^2C(z)}{d\,z^2}=\frac{\mu_{max}C(z)\,X_{f1}}{Y_{X/S}(K_S+C(z))} \quad (2).$$

To compare the number of nutrients transferred in stratified and homogeneous biofilms, we solve the equations (1) and (2). This model is predicated on the following assumptions. (i) The biofilm is a continuum. (ii) Microorganisms only consume nutrients that are transferred by diffusion. (iii) Nutrient diffusion obeys Fick's law. (iv) Only one limiting nutrient is used at a rate that the Monod equation can describe. (v) The biofilm processes occur in a pseudo-steady- state, implying that the limiting nutrient consumption rate does not vary for a short time. (vi)The transfer of the limiting nutrient only occurs in one dimension perpendicular to the substrate. (vii) Biofilms grow on inactive and impervious surfaces.

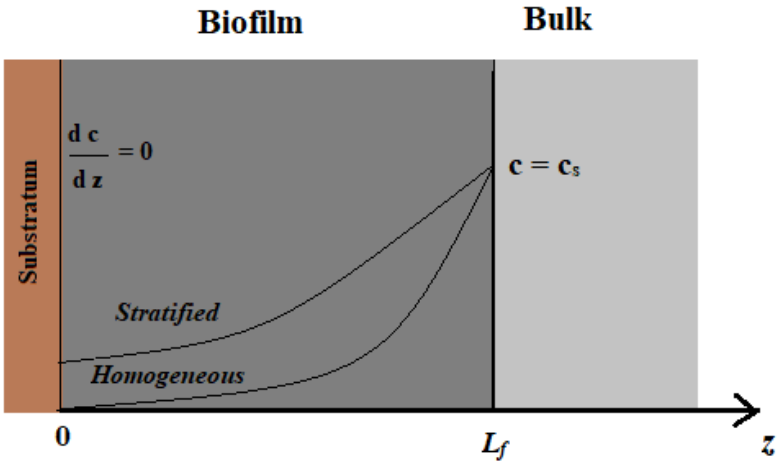

Figure 2. Schematic diagram for stratified and homogeneous biofilm model.

By defining the following dimensionless parameters,

$$z^* = \frac{z}{L_f}, C^* = \frac{C}{C_s}, \beta = \frac{K_s}{C_s}, \Psi = \frac{a}{L_f \zeta}, \Phi = \sqrt{\frac{\mu_{max} L_f^2 X_{fav}}{Y_{x/s} C_s D_{fav}}}, X_{fav} = \frac{X_{f1}}{X_f^*} \quad (3)$$

the Eq. (1) reduces to the following dimensionless form [13]:

$$\frac{d^2C^*(z^*)}{d z^{*2}} + \frac{1}{\Psi + z^*}\frac{dC^*(z^*)}{d z^*} = \frac{\Phi^2(2\Psi+1)C^*}{2X_{fav}(\Psi+z^*)(\beta+C^*)}\left[38.976\left(\frac{1+\frac{z^*}{\Psi}}{\kappa}\right)^{-0.7782} - 38.856\right] \quad (4)$$

where $\Psi\left(= a/L_f\,\zeta\right)$ represents the difference in diffusivity between the biofilm's surface and its bottom as well as its effective diffusivity, Φ is the Thiele modulus, X_{fav} is the averaged biofilm density, $\beta\ (=\ K_S/C_s)$ is the dimensionless Monod half rate constant , L_f is the average biofilm thickness, a is the effective diffusivity at the bottom of the biofilm and C_s is the denotes the biofilm's surface in terms of nutrient concentration, z^* is the dimensionless distance. Eq. (2) reduces to the following dimensionless form:

$$\frac{d^2C^*(z^*)}{d z^{*2}} = \Phi^2 \frac{C^*}{(\beta+C^*)} \quad (5)$$

The boundary conditions in dimensionless form in stratified and homogeneous biofilm may be presented as follows:

$$\text{At } z^* = 1, C^* = 1 \quad (6)$$

$$\text{At } z^* = 0, \frac{d\,C^*}{d\,z^*} = 0 \quad (7)$$

The effectiveness factor for stratified biofilms is

$$\eta_s = \frac{2\,(\beta+1)(\Psi+1)}{\Phi^2(2\Psi+1)}\left(\frac{dC^*}{d\,z^*}\right)_{z^*=1} \quad (8)$$

The homogenous biofilm effectiveness factor is

$$\eta_h = \frac{(\beta+1)}{\Phi^2}\left(\frac{dC^*}{d\,z^*}\right)_{z^*=1} \quad (9)$$

To compare the activity of stratified biofilms to that of homogeneous biofilms, we determine the ratio of their effectiveness factors(η_h/η_s).

3. APPROXIMATE ANALYTICAL EXPRESSION OF THE CONCENTRATIONS USING HYPERBOLIC FUNCTION METHOD

Recently, several asymptotic methods have been developed to solve the nonlinear differential equations, such as the Taylor series method [16-20], the Adomian decomposition method [21,22], the variation iteration method [23,24], the homotopy perturbation method [25-27], the hyperbolic function method [28-35], Pade approximation technique [36] and Rajendran-Joy method [37].

The hyperbolic function method is a simple semi-analytical method. In this method, a trial solution is assumed for the problem, and then, through a set of algebraic calculations, the constant parameters of the trial solution are determined. In comparison with other semi-analytical techniques, this method has a very simple solving process such that only the initial/boundary conditions, the main differential equations, and its derivatives are required. As a consequence, a solution with high precision will be obtained. Using this method the concentration in stratified biofilms can be obtained as follows (Appendix-A):

$$C^*(z^*) = \frac{\cosh(mz^*)}{\cosh m} \tag{10}$$

where m is the constant coefficient.

$$m^2 + \frac{m\tanh m}{\Psi+1} + \frac{\Phi^2\,(2\Psi+1)}{2\,X_{fav}\,(\Psi+z^*)(\beta+1)}\left[38.856 - 38.976\left(\frac{1+\frac{1}{\Psi}}{\kappa}\right)^{-0.7782}\right] = 0 \tag{11}$$

The unknown parameter m can be obtained by solving the equation (11) using wolframalpha.com (free software).The effectiveness factor for stratified biofilms is

$$\eta_s = \frac{2(\beta+1)(\Psi+1)}{\Phi^2(2\Psi+1)} m\tanh m \tag{12}$$

The dimensionless concentration of homogeneous biofilms becomes,

$$C^*(z^*) = \frac{\cosh\left(\frac{\Phi}{\sqrt{1+\beta}}z^*\right)}{\cosh\left(\frac{\Phi}{\sqrt{1+\beta}}\right)} \tag{13}$$

The effectiveness factor for homogeneous biofilms is

$$\eta_h = \left(\frac{\sqrt{1+\beta}}{\Phi}\right)\tanh\left(\frac{\Phi}{\sqrt{1+\beta}}\right) \tag{14}$$

s

4. RESULTS AND DISCUSSION

Equations (10) and (14) represents the new approximate analytical expression of the stratified and homogeneous biofilm. Concentration depends upon the parameters Thiele modulus, Monod half rate constant, ratio in diffusivity between the surface and the bottom of the biofilm, the relative effective diffusion coefficient, average biofilm density. Concentration of stratified biofilm $C^*(z^*)$ for various

values of parameters Φ, κ, Ψ, β, and X_{fav} using Eq. (10) is plotted in Figure 3. From this figure it is observed that concentration at the surface increases when β, and X_{fav} increases or Φ, κ, Ψ decrease.

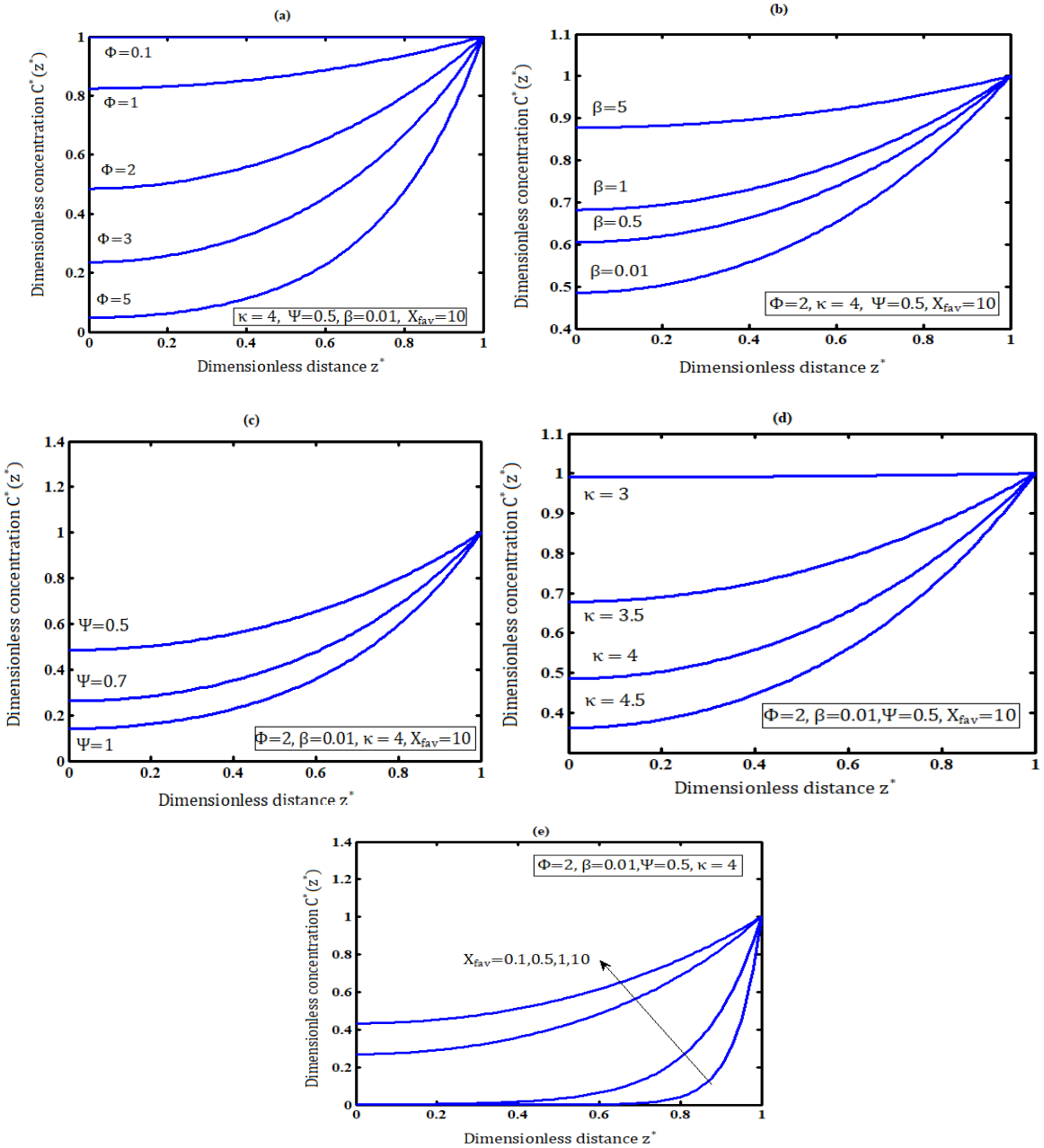

Figure 3 Dimensionless concentration of stratified biofilm $C^*(z^*)$ for various values of Φ, κ, Ψ, β, and X_{fav} using Eq. (10).

The concentration profiles of the homogeneous biofilm phase $C^*$are shown in Fig. 4(a-c) for various values of the parameters as indicated. These concentration profiles were determined using expression defined in Eq. (13). From Figs. 4. (a-c), it is inferred that the concentration of homogeneous in the biofilm phase C^*decreases when Φ decreases for different values of β. The homogeneous concentration of the biofilm phase reaches its minimum when $\beta < 0.01$ and $\Phi \leq 50$.

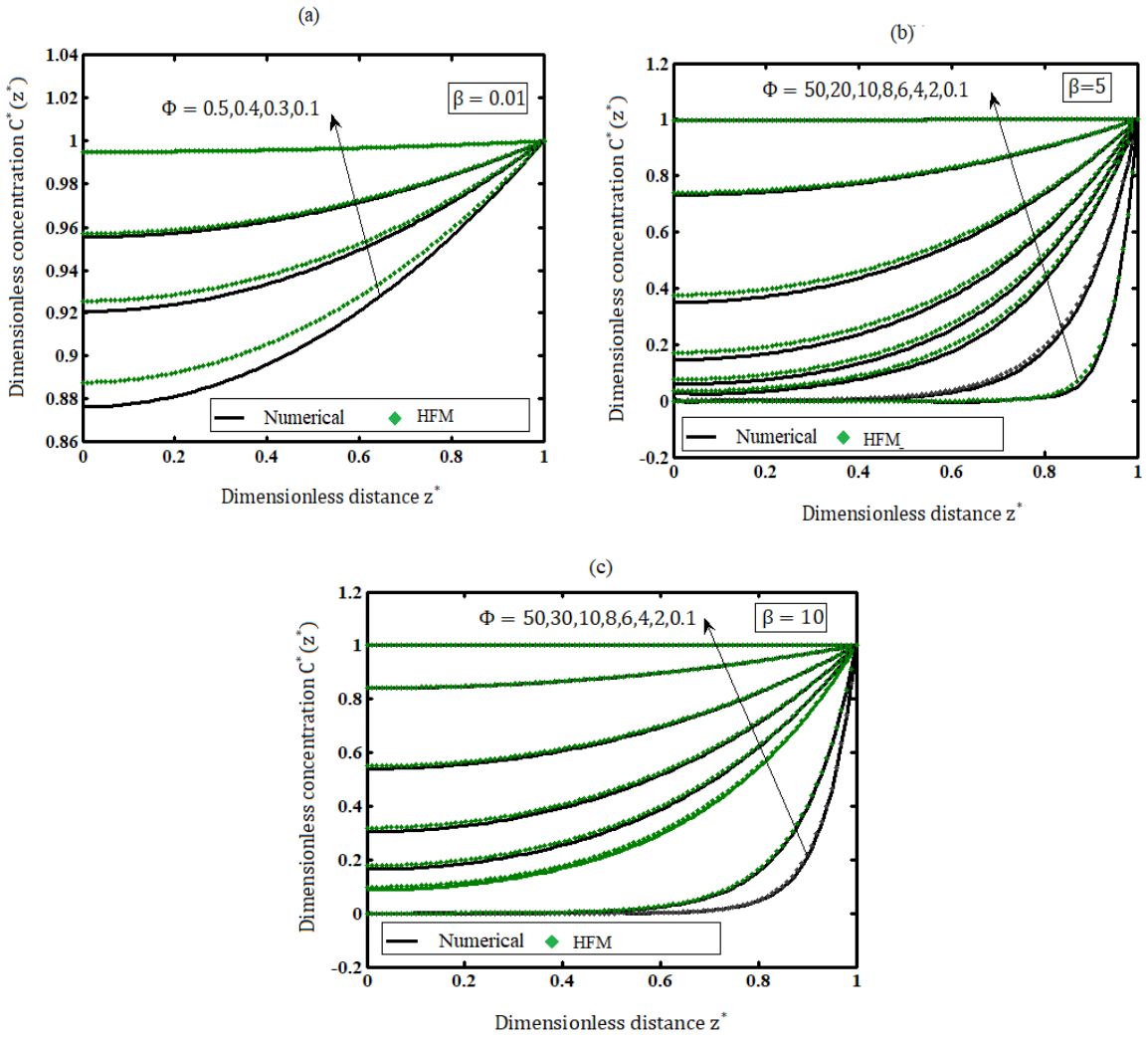

Figure 4. Comparison of analytical expression of concentration of homogeneous biofilms $C^*(z^*)$ with simulation result for various value for Thiele modulus Φ. Dotted line represent the (Eq. (13)) and solid line represent the numerical result.

Table 1. Comparison of dimensionless concentration of homogeneous biofilms $C^*(z^*)$ with simulation results for various values of parameter Φ when β=0.01.

z^*	Φ = 0.1			Φ = 0.3			Φ = 0.5		
	Numerical	Analytical Eq. (13)	Error % Eq. (13)	Numerical	Analytical Eq. (13)	Error % Eq. (13)	Numerical	Analytical Eq. (13)	Error % Eq. (13)
0	0.9950	0.9951	0.0100	0.9555	0.9557	0.0209	0.8764	0.8878	1.3008
0.2	0.9953	0.9953	0.0000	0.9573	0.9588	0.1567	0.8814	0.8923	1.2367
0.4	0.9959	0.9959	0.0000	0.9627	0.9640	0.1350	0.8966	0.9058	1.0261
0.6	0.9969	0.9969	0.0000	0.9718	0.9727	0.0926	0.9218	0.9285	0.7268
0.8	0.9983	0.9983	0.0000	0.9845	0.9850	0.0507	0.9571	0.9606	0.3657
1	1.0000	1.0000	0.0000	1.0000	1.0000	0.0000	1.0000	1.0000	0.0000
	Average error (%)		0.0017	Average error (%)		0.0760	Average error (%)		0.7760

Table 2. Comparison of dimensionless concentration of homogeneous biofilms $C^*(z^*)$ with simulation results for various values of parameter Φ when β=5.

z^*	$\Phi = 0.1$			$\Phi = 10$			$\Phi = 50$		
	Numerical	Analytical Eq. (13)	Error % Eq. (13)	Numerical	Analytical Eq. (13)	Error % Eq. (13)	Numerical	Analytical Eq. (13)	Error % Eq. (13)
0	0.9992	0.9992	0.0000	0.0304	0.0337	10.855	0.0000	0.0000	0.0000
0.2	0.9992	0.9992	0.0000	0.0350	0.0387	10.571	0.0000	0.0000	0.0000
0.4	0.9993	0.9993	0.0000	0.0759	0.0782	3.0303	0.0000	0.0000	0.0000
0.6	0.9995	0.9995	0.0000	0.1819	0.1859	2.1990	0.0000	0.0000	0.0000
0.8	0.9997	0.9997	0.0000	0.4397	0.4389	0.1819	0.0143	0.0162	13.288
1	1.0000	1.0000	0.0000	1.0000	1.0000	0.0000	1.0000	1.0000	0.0000
	Average error (%)		0.0000	Average error (%)		4.4729	Average error (%)		2.2144

Table 3. Comparison of dimensionless concentration of homogeneous biofilms $C^*(z^*)$ with simulation results for various values of parameter Φ when β=10.

z^*	$\Phi = 0.1$			$\Phi = 10$			$\Phi = 50$		
	Numerical	Analytical Eq. (13)	Error % Eq. (13)	Numerical	Analytical Eq. (13)	Error % Eq. (13)	Numerical	Analytical Eq. (13)	Error % Eq. (13)
0	0.9995	0.9995	0.0000	0.0875	0.0978	11.771	0.0000	0.0000	0.0000
0.2	0.9996	0.9996	0.0000	0.1058	0.1166	10.207	0.0000	0.0000	0.0000
0.4	0.9996	0.9996	0.0000	0.1683	0.1628	3.2678	0.0000	0.0000	0.0000
0.6	0.9997	0.9997	0.0000	0.3006	0.3032	0.8649	0.0000	0.0000	0.0000
0.8	0.9998	0.9998	0.0000	0.5556	0.5636	1.4399	0.0493	0.0476	3.4483
1	1.0000	1.0000	0.0000	1.0000	1.0000	0.0000	1.0000	1.0000	0.0000
	Average error (%)		0.0000	Average error (%)		4.5918	Average error (%)		0.5747

The nonlinear diffusion equation (5) is also solved numerically using the Matlab software. In Tables (1-3), the simulation results is compared by our analytical result for the experimental values of parameters. Values of the different dimensionless parameters used for simulation is given in Table-4. The overall maximum average error percentage between numerical and analytical results is 2.21%.

Table 4. Experimental values of parameters used for simulation .

Parameter	**Meanings**	**Beyenal [13]**	**This work (**Figs. 3-6, Tables 1-3)	**Unit**
Φ	Thiele modulus.	0 to 20.62	0 to 20.62	None
β	Dimensionless Monod half rate constant.	0.044 to 0.5	0.044 to 10	None
Ψ	Ratio in diffusivity between the surface and the bottom of the biofilm.	0.25 to 25	0.5 to 25	None
κ	The relative effective diffusion coefficient.	4	4 to 4.5	None
X_{fav}	Average biofilm density	10 to 77.8	0.1 to 77.8	g/L

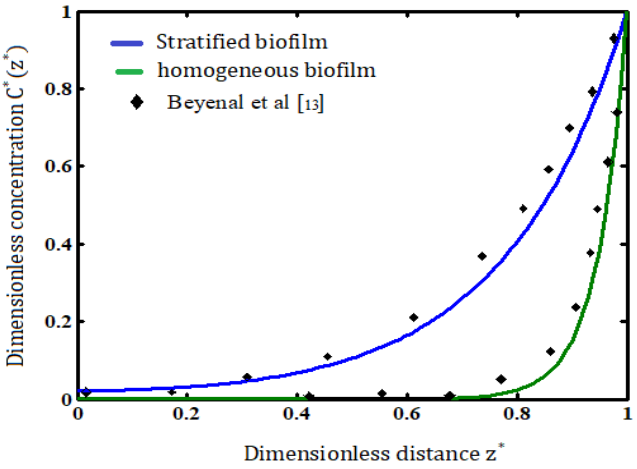

Figure 5. Comparison of analytical expressions of concentration of stratified (Eq. (10)) and homogeneous biofilm (Eq. (13)) with numerical results [13] for the experiment values of the parameter $\kappa = 4$, Φ=20.62, Ψ=0.25, β=0.125, X_{fav}=77.8. Dotted line represents numerical and solid line represent the analytical result.

Figure 5 compares the concentration profiles for homogeneous and stratified biofilm with numerical results. From the Figure, it is inferred that the concentration for stratified biofilm is always higher than for homogeneous biofilm since the growth-limiting nutrient can penetrate deeper into stratified biofilm than into homogeneous biofilms.

(i) Effect of the parameters on effectiveness factor

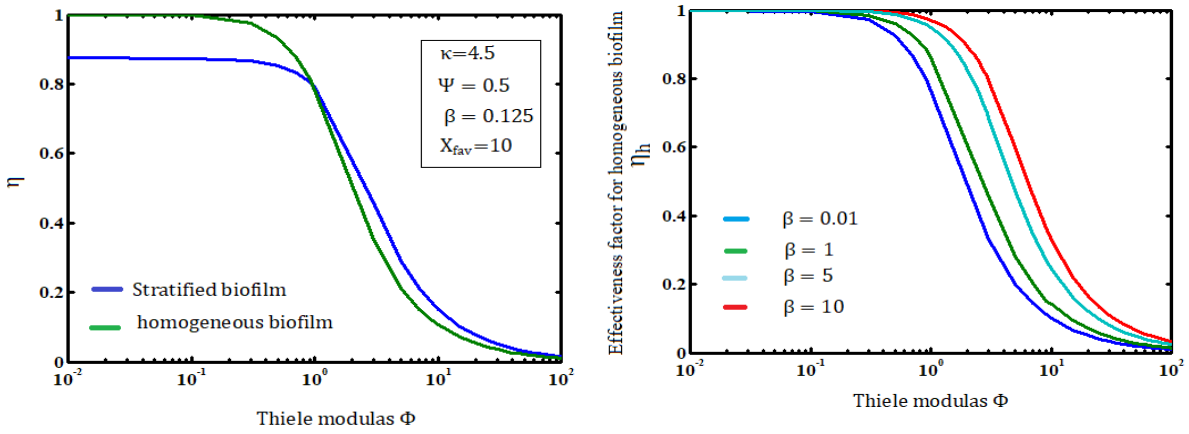

Figure 6. Comparison of effectiveness factor for stratified and homogeneous biofilm for various values of Φ and β using Eqs. (12) and (14).

The influence of parameters Φ and β on the effectiveness factor of homogeneous and stratified biofilms biofilm is shown in Figure 6. From the Figure, it is observed that when $\Phi < 1$ the effectiveness

factor is 1. Also the effectiveness factor decreases when Thiele modules increases and reaches the minimum value when $\Phi = 100$ for all values of saturation parameter (β).

We provide a new analytical method that considers continuum change in substrate effective diffusivity and biofilm density to describe stratified and homogeneous biofilm activities. Powerful experimental tools like CLSM, magnetic resonance imaging, or microsensors are frequently used in biofilm research to make observations at the microscale [38]. Such results can be interpreted using our analytical approach. The kinetics of the rate of substrate consumption and the impact of many parameters that define a stratified and homogeneous biofilm may be quickly and effectively assessed using this analytical approach.

5. CONCLUSION

The nonlinear differential equation in microbial activity has been solved analytically. In this paper, we used stratified biofilms to create a model that predicts microbial activity in heterogeneous biofilms. The hyperbolic function method is used to derive explicit solutions for the concentrations and effectiveness in homogeneous and stratified biofilms for all values of parameters. Simulated results are compared with analytical results. A significant concurrence is noticed. The influence of Thiele modules and saturation parameters on the effectiveness factor is also discussed.

Appendix A: The solution of Eq. (4) using hyperbolic function method.

Assume that the solution to Eq. (4) is of the following hyperbolic function form:

$$C^*(z^*) = A_0 \cosh(mz^*) + B_0 \sinh(mz^*) \quad \text{(A1)}$$

where A_0, B_0 and m are constant. The values of A_0 , $B_0$are found easily from boundary conditions (6) and (7), that is

$$A_0 = \frac{1}{\cosh(m)}, B_0 = 0 \quad \text{(A2)}$$

As a result, Eq. (A1) becomes

$$C^*(z^*) = \frac{\cosh(mz^*)}{\cosh(m)} \quad \text{(A3)}$$

We use the general form of Eqs. ((4) and (5)) to find the constant m in Eq. (A3).

$$F(z^*) = \frac{d^2C^*(z^*)}{d\,z^{*2}} + \frac{1}{\Psi+z^*}\frac{dC^*(z^*)}{d\,z^*} + \frac{\Phi^2(2\Psi+1)C^*}{2X_{fav}\,(\Psi+z^*)(\beta+C^*)}\left[38.856 - 38.976\left(\frac{1+\frac{1}{\Psi}}{\kappa}\right)^{-0.7782}\right] = 0 \quad \text{(A4)}$$

$$G(x) = \frac{d^2C^*(z^*)}{d\,z^{*2}} - \Phi^2\frac{C^*}{(\beta+C^*)} = 0 \quad \text{(A5)}$$

We obtain the Eqs. ((A4) and (A5)) by substituting it for Eq. (A3)

$$F(x)|_{z^*=1} = m^2 + \frac{m\tanh m}{\Psi+1} + \frac{\Phi^2\,(2\Psi+1)}{2\,X_{fav}\,(\Psi+z^*)(\beta+1)}\left[38.856 - 38.976\left(\frac{1+\frac{1}{\Psi}}{\kappa}\right)^{-0.7782}\right] = 0 \quad \text{(A6)}$$

$$G(x)|_{z^*=1} = m^2 - \frac{\Phi^2}{(\beta+1)} = 0 \quad \text{(A7)}$$

This becomes

$$m^2 + \frac{m\tanh m}{\Psi+1} + \frac{\Phi^2(2\Psi+1)}{2\,X_{fav}(\Psi+z^*)(\beta+1)}\left[38.856 - 38.976\left(\frac{1+\frac{1}{\Psi}}{\kappa}\right)^{-0.7782}\right] = 0 \quad \text{(A8)}$$

For the homogeneous biofilm

$$m = \frac{\Phi}{\sqrt{1+\beta}} \quad \text{(A9)}$$

Nomenclature

Symbols	Description	Units
a	Effective diffusivity at the bottom of the biofilm	m^2/s
A	Surface area of the biofilm	m^2/s
C	Nutrient concentration of growth-limiting	kg/m^3
C_s	Nutrient concentration at the surface of the biofilm	kg/m^3
D_{fz}	Surface averaged effective diffusivity of growth-limiting nutrient	m^2/s
D_{fa}	Average effective diffusivity of growth-limiting nutrient	m^2/s
D_{f1}	Local effective diffusivity of growth-limiting nutrient	m^2/s
K_S	Monod half rate constant	kg/m^3
L_f	Average biofilm thickness	m
X_{fav}	Average biofilm density	kg/m^3
X_{f1}	Average biofilm density in the differential element	kg/m^3
μ_{max}	Maximum specific growth rate	s^{-1}
C^*	Dimensionless concentration	None
D_{fav}	Average effective diffusivity	None
D_f^*	Dimensionless effective diffusivity	None
X_f^*	Dimensionless biofilm density	None
$Y_{x/s}$	Yield coefficient (kg microorganisms/kg nutrient)	None
z^*	Dimensionless distance	None
ζ	Effective diffusivity gradient	None
β	Dimensionless Monod half rate constant	None
η_s	Effectiveness factor for a stratified biofilm	None
η_h	Effectiveness factor for a homogeneous biofilm	None
Φ	Thiele modulus	None
κ	At the bottom of the biofilm, the inverse of the relative effective diffusion coefficient	None
Ψ	Ratio in diffusivity between the surface and the bottom of the biofilm and the effective diffusivity at the bottom of the biofilm	None

References

1. R. Bakke, R. Kommedal, S. Kalvenes, *J. Microbiol. Methods*, 44 (2001)13--26.
2. TE. Cloete, MR. Maluleke, *Water Sci. Technol*., 52 (2005) 211--216.
3. MN. Pons, K. Milferstedt, E. Morgenroth, *Biotechnol. Bioeng*., 103 (2009) 105--116.
4. A. Pereira, J. Mendes, LF. Melo, *Biotechnol. Bioeng.*, 99 (2008) 1407—1415
5. 5.GJ. Licina, G. Nekosku, RL. Howard, An electrochemical method for on-line monitoring of biofilm activity in cooling water, CORROSION/92, Paper 177, National Association of Corrosion Engineers, Houston, TX, 1992.
6. SW. Borenstein, GJ. Licina, An overview of monitoring techniques for the study of microbiologically influenced corrosion, CORROSION/94, Paper 611, National Association of

Corrosion Engineers, Houston, TX, 1994.
7. ST. Sultana, JT. Babauta, H. Beyenal, *Biofouling*. 31(9-10) (2015) 745-58.
8. B. Atkinson, I.J Davies, *Trans. Inst. Chem. Engrs*., 52 (1974) 248-259.
9. K. Williamson, P.L. McCarty, *J Water Pollut Control Fed*., 48 (197) 281–296.
10. B.E. Rittmann, P.L. McCarty, *Biotechnol. Bioeng*., 22 (1980a) 2359–2373.
11. B.E. Rittmann, P.L. McCarty, *Biotechnol. Bioeng*., 22 (1980b) 2343–2357.
12. S. W. Hermanowicz, *Math. Biosci*., 169 (2001) 1-14.
13. H. Beyenala, Z. Lewandowski, *Chem. Eng. Sci*., 60 (2005) 4337 – 4348.
14. H. Beyenal, A. Tanyolac., Z. Lewandowski, *Water Sci. Technol*., 38 (1998) 171–178.
15. H. Beyenal, Z. Lewandowski*, Biotechnol. Prog*., 18 (2002) 55–61.
16. P. Jeyabarathi, M. Kannan, L. Rajendran, *Theor. Found. Chem. Eng*., 55(5) (2021) 851-861.
17. C.H. He, Y. Shen, F.Y Ji, J.H. He, *Fractals*., 28 (2020) 1-8
18. R. Umadevi, M. Chitra Devi, K. Venugopal, L. Rajendran, MEG. Lyons, *Int. J. Electrochem. Sci*., 17 (2022) 220560.
19. K. Lakshmi Narayanan, R. Shanthi, R. Usha Rani, M.E.G. Lyons, L. Rajendran, *Int. J. Electrochem. Sci*., **17** (2022) 220623.
20. B. Manimegalai, R Swaminathan, M.E.G. Lyons, L. Rajendran, *Int. J. Electrochem. Sci*., 17 (2022) 22074.
21. P. Jeyabarathi, L. Rajendran, M. Abukhaled, M. Kannan, *React. Kinet. Mech. Catal*., 66 (2022)1-16.
22. A.U. Keskin, Springer, Cham., (2019) 311-359.
23. M. Abukhaled, *J. Math*., (2013) 1-4.
24. J.H. He, X.H. Wu, *Comput. Math. with Appl*., 54(7-8) (2007) 881-894.
25. B Manimegalai, L Rajendran, *J Electroanal Chem*., 922 (2022) 116706.
26. JH. He, YO. El-Dib, AA. Mady, *Fractal Fract*., 5(3), 93 (2021) 1-8.
27. JH. He, YO. El-Dib, *J Math Chem*., 59(4) (2021) 1139-1150.
28. P. Jeyabarathi, L. Rajendran, M.E.G. Lyons, *J Electroanal Chem*., 910 (2022).11618.
29. B. Manimegalai, M.E.G. Lyons, L. Rajendran*, J Electroanal Chem*., 880 (2021) 114921.
30. P. Jeyabarathi, L. Rajendran, Marwan Abukhaled, M.E.G. Lyons, M. Kannan, Int. J. Electrochem. Sci., 17 (2022) 22093.
31. R. Umadevi, P. Jeyabarathi, K. Venugopal, M.E.G.Lyons, L.Rajendran, *Electrochem*, 3 (2022) 361–378.
32. R. Vanaja, P. Jeyabarathi, L. Rajendran, M.E.G. Lyons, *Int. J. Electrochem. Sci*.,17 (2022) 220569.
33. R. Vanaja, P. Jeyabarathi , L. Rajendran, M.E.G. Lyons, *Int. J. Electrochem Sci*, 17 (2022) 220337.
34. S. Padma, P. Jeyabarathi, L. Rajendran, M. E. G. Lyons, Int. J. Electrochem. Sci., 17 (2022) 220336.
35. P. Jeyabarathi, L. Rajendran, M. E. G. Lyons, M. Abukhaled, *Electrochem*, 3 (2022) 699–712.
36. M. Chitra Devi, L. Rajendran, A. Bin Yousaf, C. Fernandez, *Electrochim. Acta*, 243 (2017) 1–6.
37. R Joy Salomi, L Rajendran, *J Electroanal Chem.*, 2022, 918,116429.
38. TJ. Battin, WT. Sloan, S. Kjelleberg, H. Daims, IM. Head, TP. Curtis, L. Eberl, *Nat Rev Microbiol*., 5(1) (2007) 76–81.